# PDP Researches at Hiroshima University

**Hiroshi Kajiyama, Giichiro Uchida and Tsutae Shinoda**
Advanced Display Laboratory, Graduate School of Advanced Sciences of Matter, Hiroshima University
1-3-1 Kagamiyama, Higashi-hiroshima, 739-8530, Japan
*TEL:81-82-424-4515, e-mail: kajiya@hiroshima-u.ac.jp*

**Keywords: PDP, Protective material, Luminous efficacy, VUV radiation**

.

## ABSTRACT
Hiroshima University opened the advanced display laboratory (ADL) in 2006 to specifically focus on the PDP researches. The mission of ADL is to lay the bases for the innovative PDP technologies. Our research efforts have been concentrated on the fundamental study of protective materials and phosphors, and also of the effect of protective materials with high γ emission in the high luminous efficacy. This paper briefly introduces the present status of our research activities.

## 1. INTRODUCTION
Plasma display panels (PDPs) utilize the VUV (Vacuum Ultraviolet) emission from micro-plasma. A high-efficacy PDP with 5 lm/W has been reported by Akiyama *et al* [1]. However, the discharge efficiency of PDP is still low compared to a Xe lamp and an excimer lamp. PDPs leave room for further improvement of micro-plasma generation.

A protective layer is a key component for the improvement, because it dominates firing voltage and discharge time lag through a secondary electron coefficient (γ). Recently, the high Xe content of a discharge gas has been adopted so as to improve luminous efficacy. Since it raises discharge voltage with higher Xe content, a protective layer with higher γ value, especially with higher γ by $Xe^+$ ions, has benn strongly desired.

Our research interest has been concerned with AC-PDP operated by the protective layer with a high secondary electron emission yield (high $\gamma_i$). It has been widely known that high $\gamma_i$ material is advantageous for lower breakdown voltage, and various chemically-active materials such as SrCaO have been applied to AC-PDP [2, 3]. The high $\gamma_i$ material is interesting from a plasma-physical point of view, since it may drastically change the plasma parameters such as electron temperature affecting discharge efficiency.

The discharge efficiency consists of two factors: (1) electron heating efficiency and (2) VUV emission efficiency. The high $\gamma_i$ protective layer has a possibility to improve these efficiencies due to the abundant secondary electron. In this work, SrO with high $\gamma_i$ value is employed as a protective layer. The detailed feature of SrO-panel is experimentally studied. Here, a focus of our experiment is on the evaluation of the following four factors; (1) breakdown voltage, (2) luminous efficacy, (3) electron energy, and (4) discharge-delay time.

This paper introduces two kinds of our research activities: In section 2, the impurity doped MgO with various γ coefficient by $Xe^+$,$\gamma_{(Xe)}$. It is shown that the value of $\gamma_{(Xe)}$ increases by impurity doping. The effect of various γ values on the firing voltage is measured for a 4-inch test panel. It is shown that the slight increase of $\gamma_{(Xe)}$ by an order of 0.01 reduces the firing voltage and that the reduction becomes larger at higher Xe content.

In section 3, the effect of protective materials on the sustaining voltage, luminous efficacy, electron temperatures and discharge time lag. The luminous efficacy and electron energy are measured in the case of MgO and SrO protective materials at the Xe content of 4 and 20 %. It is shown that higher luminous efficacy and lower electron energy are realized in the case of SrO due to the lower operation voltage.

## 2. Effect of Secondary electron Emission by $Xe^+$ on Firing Voltage [4]

### 2-1. Experimentals
The MgO thin films doped with some impurities were deposited on a stainless steel by electron beam evaporation. The substrate temperature and deposition rate were 523 K and 0.5 nm/s, respectively. The film thickness was 100 nm. The γ values were measured by irradiating Ne+ and Xe+ ions.

The discharge voltage was measured by setting the 4-inch PDP front and back test panels before sealing in a vacuum chamber.

The PDP discharge plasma is produced at 40~93 kPa in Ne-Xe (4%) or Ne-Xe (20%) gas by alternatively applying positive dc pulse voltage 170 ~ 300V to X and Y electrodes with respect to Y and X electrode, respectively.

### 2.3 RESULTS AND DISCUSSION
Figure 1 shows an example of $\gamma$ measured as a function of the initial injection energy of $Xe^+$. The $\gamma$ values depended on the injection energy and it consisted of a plateau Auger component and a linearly increasing component. It is suggested that the sputtering contribution was included in the kinetic process. Therefore, we adopted the $\gamma$ at the plateau values in fig. 2.

Figure 2 shows the plots of the $V_{fl}$ versus the $\gamma_{(Xe)}$ of $Xe^+$. The $V_{fl}$ depended on $\gamma_{(Xe)}$. It should be noted that even a slight increase of $\gamma_{(Xe)}$ such as an order of 0.01 reduced $V_{fl}$ and that the voltage reduction increased at higher Xe content (4%→20%).

Our measurement clearly demonstrates that the slight increase of $\gamma_{(Xe)}$ drastically reduces the $V_{fl}$ especially for high

Xe contents. This phenomenon could be explained by the dynamic behavior of $Xe^+$ and $Ne^+$ densities in PDP discharge. Before breakdown occurs, the contribution of $Xe^+$ flux to secondary electron emission is dominant compared with that of $Ne^+$ flux, because $Ne^+$ density is extremely low because of the small ionization coefficient. Once discharge is triggered, Ne ionization rapidly increases due to the appearance of sheath region with strong electric field. This dynamic feature means that $\gamma_{(Xe)}$ considerably affects breakdown voltage especially in high-Xe PDP with less $Ne^+$, even though $\gamma_{(Xe)}$ is much smaller than $\gamma_{(Ne)}$.

In conclusion, we have shown that a secondary electron yield by $Xe^+$ ions plays a significant role in the reduction for firing voltage at high Xe content gas.

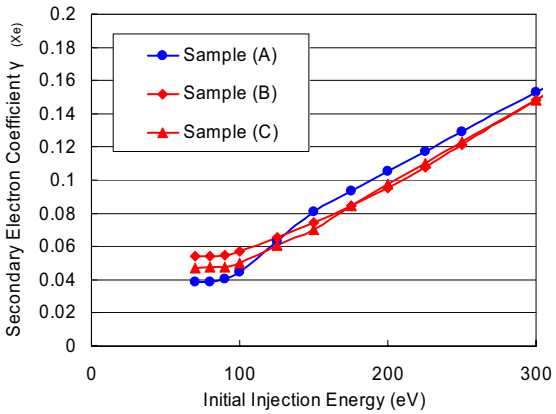


**Figure 1. The $\gamma$ measured as a function of initial injection energy of $Xe^+$ ions. The $\gamma$ values changed by doping.**

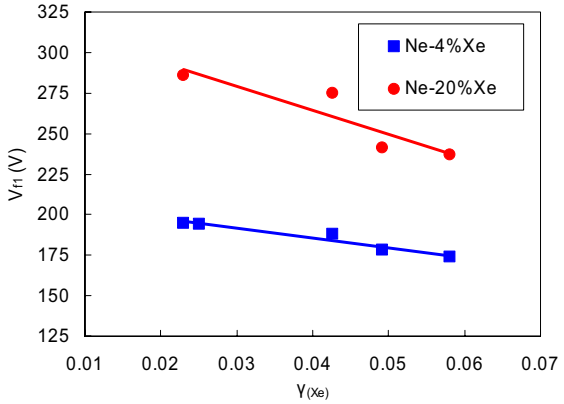


**Figure 2. The firing voltage, $V_{f1}$, as a function of secondary electron yield by $Xe^+$ ions for a gas mixture of (Ne+4% Xe) and (Ne+Xe20%). A total gas pressure was fixed at 67 kPa. The firing voltage, Vf1, is the one at which one cell first fired as the sustain voltage was gradually increased.**

## 3. Luminous efficacy and electron energy for MgO- and SrO- panel [5]

### 3.1. Experiments

#### (1) Breakdown voltage

MgO- and SrO-panels have been processed without an exposure to abundant in order to keep the MgO and SrO surface as clean as possible. A breakdown voltage was measured without sealing in a chamber filled with Ne/Xe gas mixture. The electrodes of the front panel is a standard stripe with 180 μm in width, and inter-electrode distance between the X and Y electrode is 80 μm. PDP discharge was triggered by applying the 15 kHz square sustaining voltage (Vs = 90 ~ 250 V) to the pair electrodes.

Figure 3 shows a variety of breakdown voltage during the aging process. Stable static margin was achieved immediately from the first breakdown, in spite of chemically-active SrO. This indicates that our experimental system is very good for the evaluation of PDP with a reactive protective material.

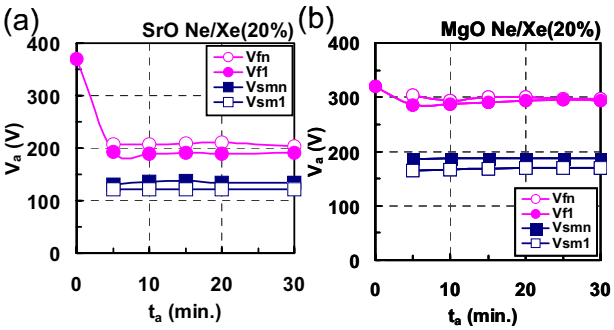


**Fig. 3. Variety of static margin during the aging process of AC-PDP with (a) SrO and (b) MgO protective layer. Stable static margin of SrO-PDP is achieved within 60 minutes.**

Table 1shows a first-cell breakdown voltage $V_{fl}$ and a minimum sustaining voltage $V_{smn}$. The breakdown voltage $V_{fl}$ of SrO-panel was as low as about 70 % with respect to that of MgO-panel. Also on the memory coefficient defined by $2(V_{fl}-V_{smn})/V_{fl}$, there is no appreciable change between SrO- and MgO-panel, ensuring normal operation of SrO-PDP. This clearly demonstrates that SrO-panel is enable to drive by the low sustaining voltage of the order of 100 V even in the high Xe concentration of 20%.

Table 1. Comparison of breakdown voltage $V_{fl}$ of (a) SrO- and (b) MgO-PDP. $V_{fl}$ of SrO-panel is as low as about 70% of that of MgO-panel.

| Gas condition | Protective layer | $V_{f1}$ (V) | $V_{smn}$ (V) | Memory coefficient |
|---|---|---|---|---|
| Ne/Xe ( 4%) 67kPa | MgO | 204 | 133 | 0.696 |
| Ne/Xe ( 4%) 67kPa | SrO | 144 | 97 | 0.653 |
| Ne/Xe (20%) 67kPa | MgO | 269-288 | 173 | 0.713-0.798 |
| Ne/Xe (20%) 67kPa | SrO | 191 | 125 | 0.691 |

#### (2) Luminous efficacy

Figure 4 and 5 show the luminance ( L) and the luminous efficacy (η)for SrO- and MgO- panel, where arrows are center of static margin, $(V_{fl}+V_{smn})/2$, of each panel. In our experiment, the SrO-panel achieved 1.5 times efficacy η with respect to ordinary MgO-panel. As shown in fig. 5, the luminous efficacy increased abruptly below 150 V corresponding to the static margin of SrO-panel; while, there is no significant change above 150 V of the operating range of MgO-panel.

This shows that the lower voltage operation of SrO-panel is more efficient (here, our experimental condition is Xe 4 %).

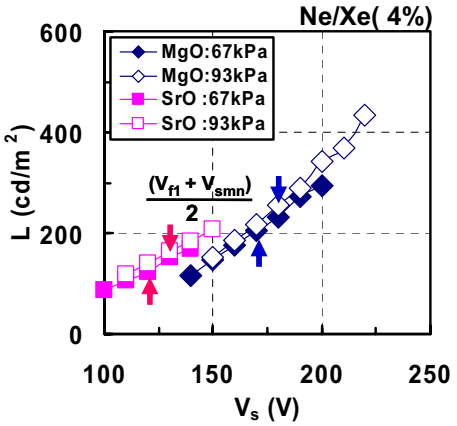


**Fig. 4. Sustaining voltage dependence of luminance L of AC-PDP for Xe concentration of 4 % at Ne/Xe gas pressure of 67 kPa, where PDPs with SrO- and MgO-protective layer are compared. Arrows show a center of static margin, $(V_{f1}+V_{smn})/2$.**

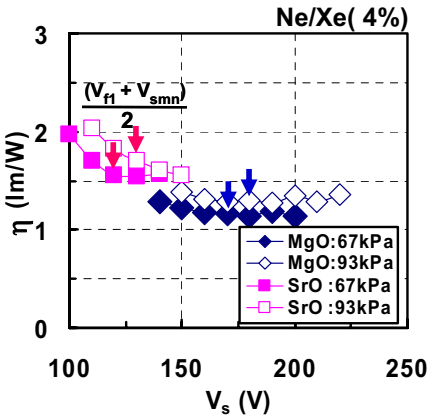


**Fig. 5. Sustaining voltage dependence of luminous efficacy ηof SrO- and MgO-PDP at Ne/Xe(4 %) gas pressure of 67 kPa. Arrows show a center of static margin, $(V_{f1}+V_{smn})/2$. The ηdrastically increases below 150 V.**

### (3) Electron energy

Figure 6 shows the relative spectrum intensity of Ne and Xe emissions $(I_{Ne(585nm)}/I_{Xe(823nm)})_{ave.}$ It was observed that it increased with $V_s$ both for SrO- and MgO-panel. This indicates that the electron energy increased proportionally to the applied voltage. By the comparison at center voltage of static margin of each panel described by arrows, it is clear that SrO-panel can be operated by the lower electron energy, which is responsible for 1.5 times higher luminous efficacy of SrO-PDP as shown in fig. 5.

Figure 7 shows the temporal evolution of relative spectrum intensity $(I_{Ne(585nm)}/I_{Xe(823nm)})$ for (a) SrO- and (b) MgO-panel at Ne/Xe(4%) pressure of 67 kPa. The arrows in this figure show the time when the Ne emission $I_{Ne(585nm)}$ reached a peak. The fraction of the Ne emission is extremely high in initial stage of discharge and drastically decreases with discharge time. This means that discharge is transient, and the electron energy exhibits a decrease with discharge time. The dynamic variety could be explained by the progress of the cathode fall from the formation to the collapse due to the charge accumulation on surface, because the electron energy is considerably sensitive to the electric field strength in the high pressure discharge such as PDP.

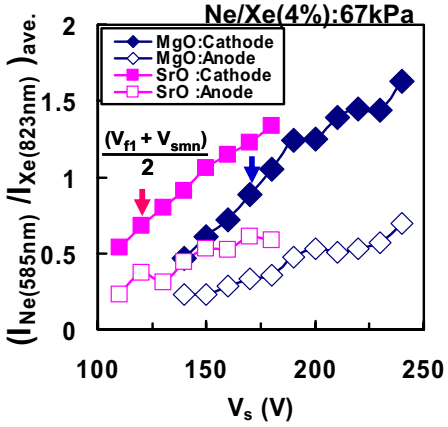


**Fig. 6. Sustaining voltage dependence of relative spectrum intensity (average) of Ne ($I_{Ne(585nm)}$) and Xe ($I_{Xe(823nm)}$) emission at Ne/Xe(4 %) gas pressure of 67 kPa. Arrows show a center of static margin, $(V_{f1}+V_{smn})/2$.**

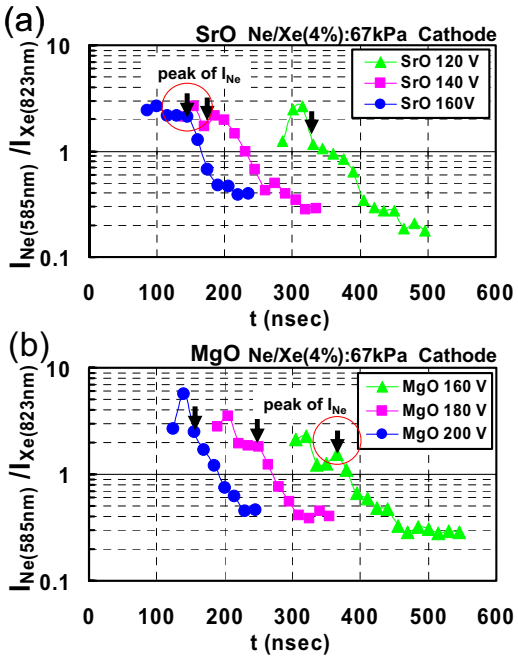

**Fig. 7. Temporal evolution of relative spectrum intensity of Ne ($I_{Ne(585nm)}$) and Xe($I_{Xe(823nm)}$) emission. (a) and (b) is SrO- and MgO-PDP, respectively. Ne/Xe(4 %) gas pressure = 67 kPa. The arrows show the timing when Ne emission has a peak. SrO and MgO panel have the different electron energy at 160 V.**

At $V_s$ = 160 V expressed by red-circles in fig. 7(a)(b), $I_{Ne(585nm)}/I_{Xe(823nm)}$ from SrO-panel is larger than that of MgO-panel. This fact suggests some effect of abundant secondary electron from SrO protective layer on electron energy, and more measurements such as ICCD observation will be performed to understand the detail of the discharge structure.

### (4) Discharge-delay time

The discharge-formation time lag ($t_d$) and the discharge-static time lag ($t_s$) (the jitter of discharge) were measured for a 20 % Xe panel. Generally, both $t_d$ and $t_s$ increase with a decrease in sustaining voltage $V_s$ as shown in fig. 8, which causes the addressing failure especially in high definition PDP. Figure 9 shows the discharge-emission signal (pink line) and the applied voltage waveform (yellow line), where about 50 emission signals are traced by the gray lines in a picture. Even though the jitter of discharge emission an be evaluated by the simple operation using a sustaining-square waveform, we can clearly find the difference between two panels. For MgO-panel as shown in fig. 9(a) and (b), the discharge-time fluctuates in the range of from 100 to about 500 nsec (*see* also fig. 8), while the discharge-time in SrO-panel was considerably stable even at a voltage as low as 130-160 V as shown in fig. 6(c) and (d) (the fluctuation range is only within 100 nsec (see fig. 8)). This result shows that the SrO-panel is advantageous also for realizing stable discharge without the jitter even though the discharge is triggered in weaker electric field.

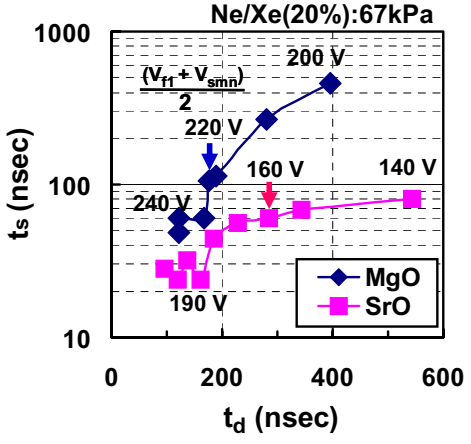


**Fig. 8. The discharge-formation-time-lag, $t_d$, and the discharge-static time lag, $t_s$, (the jitter of discharge) defined in fig. 7(a), where PDPs with SrO and MgO as a protective layer are compared. Arrows show a voltage of a center of static margin, $(V_{f1}+V_{smn})/2$, of each panel.**

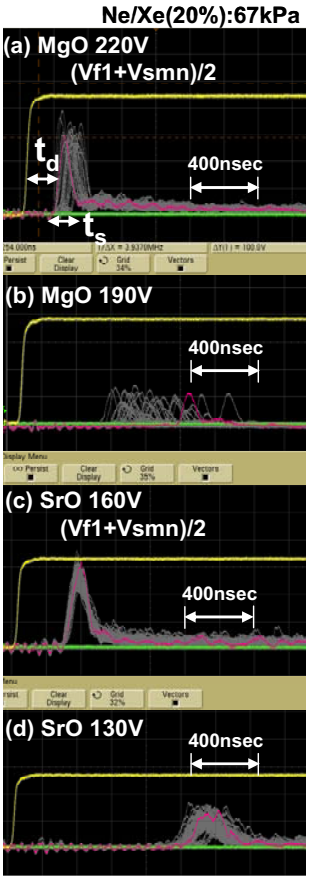


**Fig. 9. The emission signal (pink line) of discharge detected by the avalanche photodiode. 50 signals are traced by the gray lines in a picture. (a) and (b) are for MgO-PDP. (c) and (d) are for SrO-PDP. An Xe concentration is 20%.**

In summary, we have shown that the SrO-PDP operated by lower voltages achieved the higher luminous efficacy and the stable discharge, compared with MgO-PDP. For an Xe concentration of 4 %, the low-voltage operation below 150 V was more efficient. This can be explained by the efficiency of Xe excitation. That is, the lower electron energy (above bout 1 eV) is more suitable for the excitation of the Xe atom. The discharge at $V_s$ = 160 V showed the higher electron energy with respect to MgO-PDP discharge (fig. 7). This is another effect of the abundant secondary electron on PDP discharge.

## 4. References

[1] T. Akiyama *et al.*, *in Proc.* Euro Display 2007, 109 (2007).

[2] T. Shinoda *et al.*, IEEE Trans. Electron Dev. 26, 1163(1979).

[3] Y. Motoyama *et al.*, Euro Display 2005, 205 (2005).

[4] M. Kitagaki *et al.*, IDW07, 213(2007).

[5] G. Uchida *et al.*, SID Symposium Digest, 1762(2008).